

Assessing capability of semiconductors to split water using ionization potentials and electron affinities only†

Cite this: *Phys. Chem. Chem. Phys.*, 2014, 16, 3706

Vladan Stevanović,^{*ab} Stephan Lany,^b David S. Ginley,^b Willam Tumas^b and Alex Zunger^c

Received 31st July 2013,
Accepted 5th November 2013

DOI: 10.1039/c3cp54589j

www.rsc.org/pccp

We show in this article that the position of semiconductor band edges relative to the water reduction and oxidation levels can be reliably predicted from the ionization potentials (IP) and electron affinities (EA) only. Using a set of 17 materials, including transition metal compounds, we show that accurate surface dependent IPs and EAs of semiconductors can be computed by combining density functional theory and many-body GW calculations. From the extensive comparison of calculated IPs and EAs with available experimental data, both from photoemission and electrochemical measurements, we show that it is possible to sort candidate materials solely from IPs and EAs thereby eliminating explicit treatment of semiconductor/water interfaces. We find that at pH values corresponding to the point of zero charge there is on average a 0.5 eV shift of IPs and EAs closer to the vacuum due to the dipoles formed at material/water interfaces.

1 Introduction

Since the first demonstration of hydrogen production *via* electrochemical photolysis of water by Fujishima and Honda¹ about 40 years ago, we still have not found a semiconductor material that can accomplish light absorption, charge separation and transfer of the photo-generated charge carriers into an electrolyte solution to split water, in an efficient and relatively inexpensive device.^{2–4} Hydrogen is an important alternative to conventional fuels and the challenge of developing technology for inexpensive, large-scale and renewable photo-electrochemical hydrogen production triggered numerous efforts in searching for viable material solutions (see ref. 5–25 and the references therein).

Whatever the approach to the water splitting problem is, the most important piece of information that makes a semiconductor a potential candidate for water splitting is the magnitude of its band gap and the position of its band edges relative to the water reduction and oxidation levels. In a device, the resulting band edges (single material or combination of several materials stacked together) have to straddle the two water levels as shown in Fig. 1 so that it is energetically favorable for the photo-generated charge carriers to leave the material and split water. The optimal band gap needs to be around $\sim 2 \text{ eV}^3$ to allow

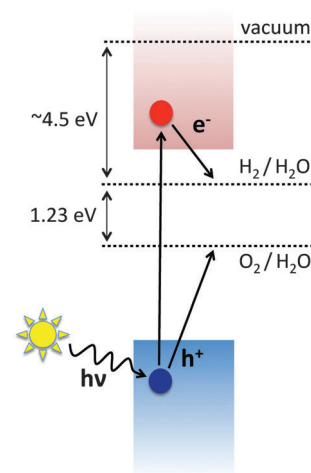


Fig. 1 Schematics of the position of electronic bands of a semiconductor material, relative to the water reduction ($\text{H}_2/\text{H}_2\text{O}$) and oxidation ($\text{O}_2/\text{H}_2\text{O}$) levels, needed for the spontaneous water splitting to occur under solar illumination. The valence band is shown in blue and the conduction band in red.

for the electrons and holes to overcome kinetic barriers while still capturing significant portion of the solar spectrum.

We show in this article that a reliable prediction of the position of the semiconductor band edges relative to the two water levels can be done solely on the basis of the ionization potentials (IP) and electron affinities (EA). First, we demonstrate on a set of 17 materials, including transition metal compounds,

^a Colorado School of Mines, Golden, CO, USA. E-mail: vstevano@mines.edu

^b National Renewable Energy Laboratory, Golden, CO, USA

^c University of Colorado Boulder, USA

† Electronic supplementary information (ESI) available. See DOI: 10.1039/c3cp54589j

that quantitatively accurate surface dependent IPs and EAs can be computed by correcting density functional theory with accurate many-body GW calculations. Second, by comparing positions of the band edges of the same materials derived from IPs and EAs with those measured electrochemically and expressed at the pH value corresponding to the point of zero charge (PZC), we find that there is on average a 0.5 eV shift of the calculated band edges closer to the vacuum due to the interaction with water molecules at the interface. This result allows direct alignment of the semiconductor band edges with water redox potential just on the basis of known IPs and EAs eliminating explicit calculations of semiconductor/water interfaces. In this way an efficient, reliable and computationally relatively simple procedure can be constructed and used in searching for new water splitting materials.

Our computational approach includes accurate many-body GW calculations for the electronic structure of bulk materials in combination with density functional theory (DFT) calculations of the corresponding surface (slab) systems for the purpose of obtaining the absolute (vacuum) reference energy, resulting in accurate, and surface orientation dependent, IPs and EAs of semiconductors and insulators. The power of this approach is in its broad applicability across the periodic table, which is enabled by employing recent developments that allow application of the GW calculations to transition metal compounds²⁶ which are known to be rather challenging for the *ab initio* based methods.

In recent years there have been an increasing number of efforts in applying computational approaches in searching for new candidate materials for water splitting.^{11–15,27} These include searching for the appropriate dopants in anatase TiO₂,¹¹ alloy compositions in ternary CoX₂O₄ (X = Al, Ga, In) space or high-throughput searches across large groups of compounds such as cubic perovskites^{13,14} or oxynitride compounds.¹⁵ In these studies the prediction of the position of the band edges relies on assumptions that, in our view, cannot be generalized to account reliably for any system. For example, to overcome the DFT band gap problem the authors of ref. 11 use a scissor operator, which attributes the whole band gap error to the conduction band, which, as we find, does not hold in general. The authors of ref. 13 and 14 use the empirical method based on atomic Mulliken electronegativities⁹ to predict the band edge positions, which, as we also show here, in many cases provides reliable predictions, but fails for two p-type oxides Cu₂O or NiO, for which the predicted band edges are too high relative to the electrochemical measurements by as much as ~1.2–1.8 eV. Furthermore, the authors of ref. 15 and 27 perform explicit calculations of the material/water interface and compute directly using DFT the position of the semiconductor conduction band minimum (CBM) relative to the LUMO level of the H₃O⁺ molecule in water. First, the underlying assumption is that the DFT band gap errors existing both in the calculated CBM of the semiconductor and the LUMO level of H₃O⁺ cancel to a good approximation. This may be the case for some materials, but as we find in our work does not hold in general as the DFT band gap error distribution among the VBM and the CBM is highly material dependent. Second is the surface orientation and termination dependence of the results. The authors of

ref. 15 and 27 provide little or no explanation which surface orientation and/or termination they use to construct the material/water interface. As we show in this paper, it is the lowest energy surface orientations and terminations that are the most relevant for the position of the band edges (as expected), which means that in complex and relatively poorly characterized systems (e.g. oxynitrides) the search for the lowest energy surface orientation and/or termination becomes essential.

2 Computational approach to ionization potentials and electron affinities of semiconductors and insulators

We compute the IPs and EAs of semiconductors and insulators by applying methodology for referencing bulk electronic levels to the vacuum that involves both bulk calculations and the surface/slab calculations. This approach has been employed previously for computing work functions of metals^{28,29} and ionization potentials of semiconductors.³⁰ Namely, the main problem is that in bulk calculations the whole space is filled with periodic crystals and the absolute energy reference, *i.e.* the vacuum level, cannot be defined. The electronic eigenvalues are typically referenced to the average electrostatic potential (ionic plus Hartree). In order to establish the absolute reference the 3D periodicity has to be destroyed and one way of doing that is by cutting out the surface or the slab. The vacuum level is then defined far away from the surface and the “bulk” average electrostatic potential as the value of the locally (macroscopically) averaged electrostatic potential deep inside the slab (see Fig. 2, Step 2). In that way the surface orientation dependent potential step ΔV between the vacuum and the bulk is established and the bulk electronic eigenvalues can be referenced to the vacuum.

The method of choice for these kind of calculations has typically been one of the standard approximations to DFT, *i.e.* the local density (LDA) or the generalized gradient approximation (GGA). However, two problems occur: (i) because of the

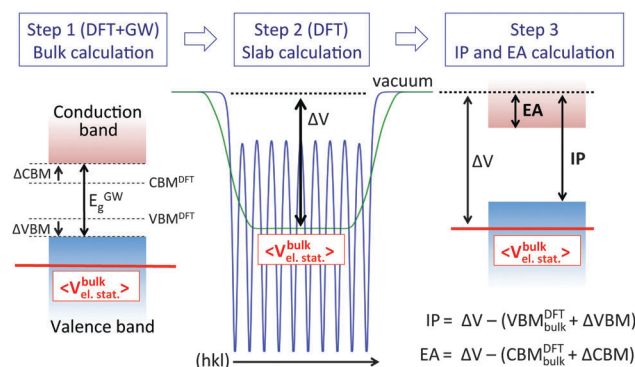


Fig. 2 Steps in the procedure adopted in this work for computing accurate ionization potentials (IPs) and electron affinities (EAs) of semiconductors and insulators. Blue curve in Step 2 represents the in plane averaged electrostatic potential of a slab defined by (hkl) Miller indices, whereas its local (macroscopic) average is shown in green.

notorious band-gap problem both in LDA and GGA the IPs of semiconductors and insulators appear to be too small and EAs too large,³⁰ and (ii) electronic structure of compounds containing d-electron metals are not reliably reproduced in both LDA and GGA. We developed a three step approach, shown schematically in Fig. 2, that deals successfully with both of these issues.

2.1 Step 1 – bulk calculations

For each of the 17 compounds studied here we start with a standard GGA + U ³¹ calculations of the bulk system, by relaxing all degrees of freedom including volume, cell shape and atomic positions. The numerical setup employed is the same as the one described in detail in ref. 32 with $U = 3$ eV for all transition metals, except Cu for which $U = 5$ eV. These U values provide a good description of the thermochemical properties³² and improve the hybridization between the d states of transition metals with the O-p ligands, which is important when the wave functions of the initial GGA + U calculations are maintained during the subsequent GW calculation. The spin degrees of freedom are included explicitly in the case of NiO, MnO and Fe₂O₃. Known antiferromagnetic spin ground states have been used for all three compounds (see ref. 26).

Subsequently, the many body GW calculations are performed using the GGA + U relaxed structures. The GW electronic eigenenergies are iterated to self consistency while the GGA + U wavefunctions are kept fixed. In this way the dependence of the results on the starting GGA + U band energies is removed and calculations are kept at reasonable computational cost. Moreover, by keeping the wave functions fixed the charge density and the resulting average electrostatic potential remain constant during the GW iterations, *i.e.* the GW eigenenergies are expressed relative to the same reference as those from GGA + U . This allows us to compute both the GW band gaps and the individual GW shift for each band edge. These shifts, denoted as $\Delta\text{VBM} = \text{VBM}^{\text{GW}} - \text{VBM}^{\text{DFT}}$ and $\Delta\text{CBM} = \text{CBM}^{\text{GW}} - \text{CBM}^{\text{DFT}}$, are shown in Fig. 2.

The local field effects are included in the GW at the level of the adiabatic-LDA approximation within time-dependent DFT.³⁴ In the case of transition metal compounds, we employ, within the GW self consistent loop, external V_d potentials acting on transition metal d-orbitals introduced by Lany,²⁶ which are shown to improve significantly the description of the electronic structure of transition metal compounds and provide accurate band gaps of these “problematic” systems. Following ref. 26 we refer to these calculations as the GW + V_d . All calculations, including those in the Step 2 and 3, are performed using the VASP computer code.³⁵

As the first test we compare the calculated band gaps of the 17 compounds with the experimental values as shown in Fig. 3. These compounds go from standard semiconductors (*e.g.* GaAs or CdS) to transition metal compounds spanning a range of band gaps from medium ~ 1.2 eV to relatively large ~ 3.6 eV. All experimental values are reproduced with the same accuracy, most of which fall between 0.1–0.2 eV from the experimental values, with maximal deviation close to 0.3 eV for GaP and Fe₂O₃.

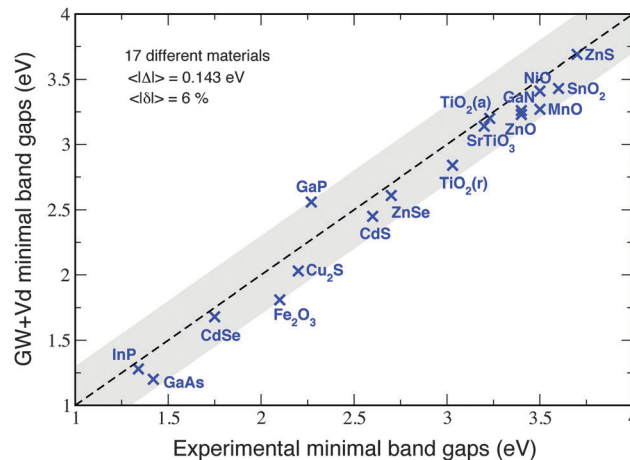


Fig. 3 Comparison of the computed minimal band gaps (GW + V_d) and those measured in experiments. Numerical values are given in the ESI.† Experimental data compiled from the Landolt–Börnstein Database³³ for standard semiconductors and from ref. 26 for transition metal compounds. Mean absolute error $\langle |Δ| \rangle$ and mean relative error $\langle |\delta| \rangle$ are also given.

2.2 Step 2 – slab calculations

In the second step the slab calculations are performed with exactly the same GGA + U setup as the one used for the initial bulk calculations. We use the supercell slab geometry with symmetric slabs constructed from the fully relaxed unit cells from the Step 1. In Fig. 2 (Step 2) the in-plane averaged electrostatic potential (blue curve) of a slab perpendicular to a given (hkl) direction is shown together with its local (macroscopic) average (green). The macroscopic average defines the potential step ΔV between the bulk (value in the middle of the slab) and the vacuum (value far away from the slab). In our calculations ΔV is converged to ~ 30 meV both with respect to the slab thickness and the thickness of the vacuum region separating periodically repeated slabs. For several specific cases (*e.g.* rutile TiO₂ or ZnO) we tested convergence of our results up to slab thicknesses of ~ 100 Å and size of the vacuum region of ~ 50 Å.

We consider only low index and non-polar surfaces as those are typically low energy surfaces that are likely not to reconstruct.^{41,42} For the systems under investigation here, the low energy and non-polar surfaces are known from the literature (*e.g.* in ref. 41–43). Miller indices of the surfaces considered in this work are provided in ESI.†

In the case of a stoichiometric SrTiO₃(001) slab, however, there are always two terminations appearing on opposite sides, *i.e.* one side is always SrO terminated and the other TiO₂ terminated. This asymmetry leads to a dipole field across the slab and the problem occurs at which point one should measure ΔV . This situation we resolve by constructing two symmetric, but off-stoichiometric slabs, one with both sides SrO terminated (SrO rich) and the other with both sides TiO₂ terminated (TiO₂ rich). In this way we can compute IPs and EAs of individual (001) terminations as both SrO and TiO₂ layers are charge-compensated, *i.e.* the off-stoichiometry does not

introduce electrons or holes into the conduction or the valence band, thereby allowing the ΔV to be computed in a relatively accurate way.

As a byproduct of the slab calculations we are able to compute surface energies, which are defined as the total energy difference between the slab and the equivalent bulk per unit of surface area:

$$E_{hkl} = \frac{E_{\text{slab}} - E_{\text{bulk}}}{2A} \quad (1)$$

Values of surface energies for all surfaces considered in this work correspond well to those available in the literature and are also given in ESI†. For SrTiO₃(001) we report the average surface energy for the two terminations computed for the asymmetric slab.

2.3 Step 3 – IP and EA calculation

After completing Step 1 and Step 2 it is possible to align bulk band edges, resulting from the bulk GW calculations, with vacuum levels using the potential steps resulting from the GGA + *U* slab calculations. Since the GW is a real quasi particle theory, the distances between the vacuum and the materials' band edges are interpreted as the IPs and EAs. A similar approach, *i.e.* using the GW method for the bulk Δ VBM and Δ CBM in combination with the DFT calculations for computing potential steps, has been employed successfully in the context of band offsets and is shown to significantly improve accuracy of the results.^{44–46} Rationale behind this approach is that the potential steps at the interfaces, both material/material and material/vacuum, can be approximated by DFT as they depend primarily on the charge distribution, which is the ground state quantity and hence little affected by many-body effects.^{44,45} Although, this work builds on previous knowledge that GW

improves significantly calculated band-offsets between two semiconductors, it is for the first time that the performance and accuracy of such calculations are assessed on a relatively large set of compounds.

Comparison with the photoemission data. The VBM and CBM positions relative to the vacuum level, derived for the calculated IPs and EAs, are provided in Fig. 4. For comparison we include available photoemission data. In the case of GaN and SrTiO₃ ranges of values can be found in the literature, which reflect sensitivity of the measurements on the surface preparation. To our knowledge, the photoemission data reporting IPs and EAs for TiO₂ (both rutile and anatase), MnO, NiO, and Fe₂O₃ are missing from the literature. For the remaining 12 compounds (GaN, GaAs, GaP, InP, SnO₂, ZnO, ZnS, ZnSe, CdS, CdSe, Cu₂O and SrTiO₃) the accuracy of the calculated IPs and EAs, when taken for the lowest energy surface orientations, is practically the same as for the band gaps, in the range of ~ 0.3 eV, similar to the performance of GW methods in reproducing measured IPs and EAs of atoms and molecules (see ref. 47 and the references therein). The fact that the most stable surfaces (with lowest surface energy) compare best with the experimental data reflects the fact that the low energy surfaces, such as (110) in the case of rutile TiO₂ or SnO₂, are most likely to be exposed in the most significant fraction in real samples. It is important to note that often the well established experimental data³³ are reported for not very well characterized surface orientations, *e.g.* stating only that the samples are cleaved.⁴⁸ In these cases experimental results correspond to IPs and EAs averaged over different surface orientation with the largest contribution coming from the lowest energy ones.

In the case of SrTiO₃ the calculated IPs and EAs of the two terminations, namely SrO and TiO₂, differ as much as 2.3 eV as

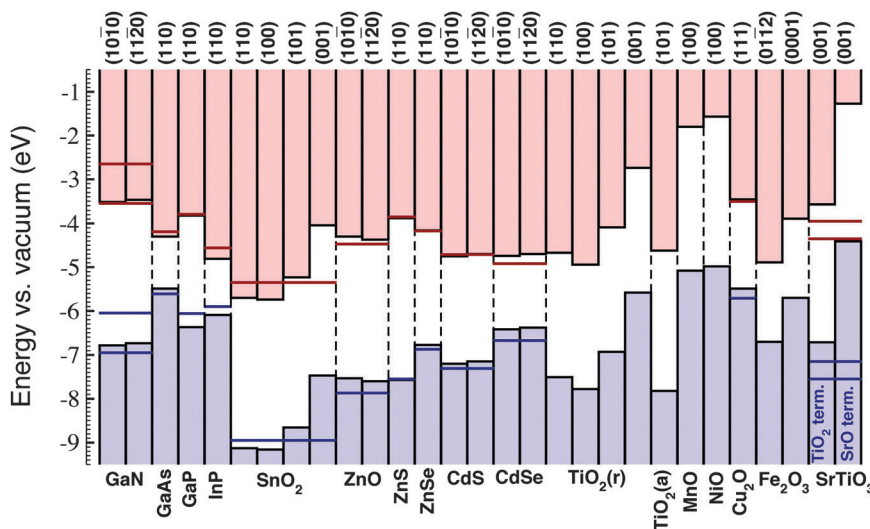


Fig. 4 Calculated band edge energies relative to the vacuum, derived from the calculated IPs and EAs, of 17 materials (values provided in ESI†). Valence bands are shown in blue and conduction bands in red. Dashed lines delineate different chemical systems (formulae shown below). Results corresponding to different surface orientations for a given material are represented with different bars with the Miller indices given on top of each bar. Whenever there is more than one surface orientation for a given material, the surfaces are arranged from left to right according to increasing surface energy. The results are compared against VBMs (bold blue lines) and CBMs (bold red lines) measured in photoemission (data from ref. 33, 36–40 and 69 provided in ESI†).

shown in Fig. 4. The VBM and CBM of SrO terminated SrTiO₃(001) surfaces are calculated to be by 2.3 eV closer to the vacuum than the IP and EA of the TiO₂ terminated surface. This is not surprising as the differences between the calculated values for pure TiO₂, both rutile (IP = 7.51, EA = 4.67) and anatase (IP = 7.82 eV, EA = 4.62), and estimated ones for SrO (EA = 0.64 eV⁴⁹)‡ are of the same magnitude. It is frequently observed in experiments that SrO termination appears to be in relatively small fraction, *i.e.* as terraces, on mostly TiO₂ terminated (001) surfaces.^{50,51} However, our calculated IPs and EAs for the TiO₂ termination correspond less accurately with the well accepted value of the work function of SrTiO₃(100) surfaces between 4.1–4.5 eV.^{39,40,52–54} Possible explanation for this discrepancy can be band bending at the surface due to the existence of the 2D electron gas regardless of the growth conditions.⁵⁵

Discussion of the calculated GW band edge shifts. We find that having GW band edge shifts ($\Delta\text{VBM} = \text{VBM}^{\text{GW}} - \text{VBM}^{\text{DFT}}$ and $\Delta\text{CBM} = \text{CBM}^{\text{GW}} - \text{CBM}^{\text{DFT}}$) is essential for obtaining accurate IPs and EAs of semiconductors and insulators. Namely, the magnitudes of ΔVBM and ΔCBM can be as large as 1.5 or 1.3 eV for ΔVBM of ZnS and ΔCBM of NiO, respectively. As shown in the figure in ESI† the band gap error, summing up to $\Delta\text{VBM} + \Delta\text{CBM}$, in most cases is not distributed evenly. The two shifts often have opposite signs, but on average ~60–70% of the error is corrected by the VBM shifts and only about ~30–40% by ΔCBM . This is also the case for standard semiconductors such as GaAs ($\Delta\text{VBM} = -0.66$ eV, $\Delta\text{CBM} = 0.33$ eV) or CdS ($\Delta\text{VBM} = -1.19$ eV, $\Delta\text{CBM} = 0.15$ eV). Furthermore, for GaP ($\Delta\text{VBM} = -1.08$ eV, $\Delta\text{CBM} = -0.01$ eV) and InP ($\Delta\text{VBM} = -0.98$ eV, $\Delta\text{CBM} = -0.17$ eV) both shifts are negative and their magnitude implies that the GGA band gap errors in these two systems can be attributed mostly to the too high VBM position (relative to the vacuum). These results imply that using the scissor operator, which attributes most of the band gap error to the conduction band, is not well founded and cannot be used for calculating IPs and EAs of semiconductors and insulators.

The same conclusions hold for the transition metal compounds. The VBM and CBM band edge shifts, now calculated within GW + V_d and defined relative to GGA + U , are close in magnitude for TiO₂, MnO and Cu₂O, but differ substantially for NiO, Fe₂O₃ and SrTiO₃. Interestingly, for Fe₂O₃ the values of the GGA + U and GW band gaps are exactly the same 1.81 eV (*versus* the experimental ~2.1 eV), as the two band edge shifts are equal and amount to -0.60 eV. The results for transition metal oxides obtained in this work have two important implications: (i) the external potentials V_d introduced in ref. 26 for the purpose of correcting the GW band gaps of transition metal oxides have a deeper physical meaning and do lead to significantly improved IPs and EAs of these systems and (ii) the assumption that the absolute position of the mid-gap energy as calculated by DFT should remain fixed after introducing many-body corrections⁵⁶ obviously does not hold in our approach neither for standard semiconductors nor for transition metal oxides.

‡ These estimations are based on measured values of other alkaline earth oxides, *e.g.* EA(CaO) = 0.70 eV and EA(BaO) = 0.57 eV.

3 IPs and EAs of semiconductors and insulators and their relation to the position of the band edges in an aqueous environment

3.1 Direct comparison of the calculated VBM and CBM positions and those measured in electrochemistry

In Fig. 5 we add to the calculated VBM and CBM positions from Fig. 4 the water reduction and oxidation levels, H₂/H₂O and O₂/H₂O, respectively, and the VBM and CBM positions measured electrochemically. Both H₂/H₂O and O₂/H₂O levels are given for a value of pH = 1, as done also for the experimental VBM and CBM positions.^{5,6,8,20,57} The agreement between two sets of data is, as expected, less quantitative than the comparison shown in Fig. 4. For 14 out of the 17 compounds computed VBM and CBM positions fall within ~0.6 eV from the experimental values. The disagreement is larger for ZnSe (~1 eV) and the experimental results are, to our knowledge, missing from the literature for ZnS and MnO.

For GaN calculated VBM and CBM fall within the range of the values reported in experiments, and based on calculations GaN would correctly be predicted to be the material that can be used for overall water splitting (both reactions).⁶² Similarly, VBM of GaAs agrees with experimental values, whereas its CBM is 0.22 eV below the experiment, which reflects that the band gap error of ~0.2 eV is still present in our calculations. For both GaP and InP, computed band edges are by ~0.2–0.6 eV below the measured ones. Consequently, the prediction would be that GaP is a good material for both H₂ and O₂ reactions, *i.e.* both as photocathode and photoanode, respectively, whereas InP can be used only for O₂ evolution, which contradicts the experimental facts that only H₂ evolution has been demonstrated on GaP⁶³ and InP can be used for both reactions if the appropriate catalysts are employed.⁶⁴ However, if the prediction based on calculated IPs and EAs is made to account for the ~0.3 eV range below and above the H₂/H₂O and O₂/H₂O levels, both GaP and InP would correctly be suggested as the potential candidate materials. Moreover, just by considering IPs and EAs of these two compounds one could also propose their alloy at 50% concentration as a candidate material, in agreement with known experimental facts,^{16,23} just by assuming that the IP and EA will be in the middle between the end points. Similarly, conclusions that are in agreement with known experimental facts can be made just on the basis of calculated IPs and EAs for ZnO and GaN/ZnO alloys, TiO₂, NiO, Cu₂O, Fe₂O₃, and SrTiO₃. For ZnSe and CdS, however, disagreements between the calculated VBM and CBM and those from electrochemistry differ more significantly. While in the case of ZnSe the experimental numbers are found only in ref. 5, for CdS two references, ref. 8 and 20, differ considerably, by as much as ~1.4 eV. In ref. 3 however, CdS is considered as a material that can drive the full water splitting suggesting that the truth is somewhere in between, probably closer to the larger values of IP and EA,

§ GaN is not stable in water though.

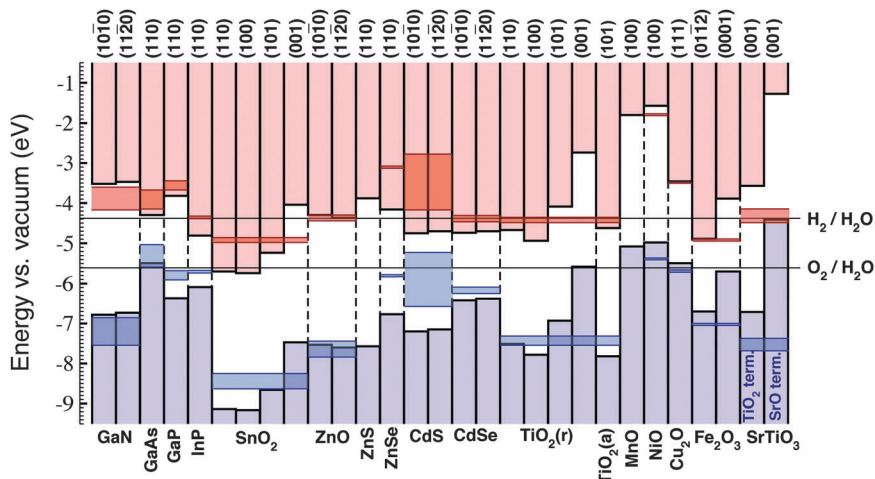


Fig. 5 Calculated band edge energies of 17 different materials as in Fig. 4 and their comparison to the ranges of electrochemically measured positions of the valence bands (blue shaded areas) and conduction bands (red shaded areas). Numerical values from ref. 5, 6, 8, 20 and 57–61 are provided in ESI†

i.e. those reported in ref. 8. Just by comparing the calculated VBM and CBM positions relative to the vacuum level and the band edges from electrochemical measurements expressed at pH = 1, it can be concluded that in all cases, except ZnSe, a reliable assessment can be made of whether a given material can be considered candidate material for water splitting.

3.2 Analysis of the relation between calculated VBM and CBM positions and those measured in electrochemistry

Given the pH dependence of electrochemical results and the fact that there is no pH dependence in the material/vacuum calculations, the question is why would one make comparison taking the experimental data at pH = 1 and not at pH = 7 or any other value, and what is the reason that some experimental band edges at pH = 1 correspond well with the calculations or photoemission data (*e.g.* ZnO, TiO₂, Cu₂O) and others do not?

First, as described by Butler and Ginley⁹ the comparison between VBMs and CBMs derived from IPs and EAs, and the data from electrochemical measurements have to be done at the pH values, which correspond to the zero net charge at the surfaces, *i.e.* the points of zero charge (PZC) or points of zero zeta potential (PZZP). Namely the following relation connecting the material/vacuum and material/water CBM positions can be written for n-type semiconductors (analogously for the p-type):

$$\text{CBM}_{\text{material/vacuum}} = V_{\text{fb}} + \Delta_{\text{fc}} + \Delta_{\text{pH}} + \Delta_{\text{dipole}} \quad (2)$$

V_{fb} is the flat band potential of a material, a quantity that is directly measured in electrochemistry, expressed on an absolute scale relative to the vacuum. The flat band potential is actually the Fermi energy of a material in water with the applied bias at which no band bending occurs. Δ_{fc} is the difference between the semiconductor Fermi energy and its CBM. Δ_{pH} describes the potential drop across the double layer due to H⁺ and OH⁻ adsorption on the surface. It is Δ_{pH} that is responsible for the pH dependence of the position of the band edges in water and its pH dependence can be approximated by the Nernst equation, *i.e.* 59 meV shift closer to vacuum per unit

of pH. Δ_{dipole} is the potential drop because of interface dipoles that develop due to the interaction of a semiconductor material with H₂O molecules. Therefore, the difference between our calculated CBM positions derived from EAs and the CBMs measured electrochemically,[¶] which are nothing but $V_{\text{fb}} + \Delta_{\text{fc}}$, equals to $\Delta_{\text{pH}} + \Delta_{\text{dipole}}$. At the PZC, which is by definition the material related pH at which $\Delta_{\text{pH}} = 0$, this difference is only due to the interface dipoles measured by the Δ_{dipole} term.

In ref. 9 Butler and Ginley demonstrated on a set of 11 oxides that there is a correlation between the EAs, estimated using atomic Mulliken electronegativities, and measured V_{fb} (as $\Delta_{\text{fc}} \sim 0.1$ eV for n-type materials, it is neglected). In this approach the electron affinity of a material is defined as:

$$\text{EA} = \chi - \frac{1}{2}E_{\text{g}} \quad (3)$$

with χ being the material electronegativity defined as the geometric mean of the electronegativities of the constituent atoms (*e.g.* $\chi(\text{TiO}_2) = [\chi(\text{Ti})\chi^2(\text{O})]^{1/3}$), and E_{g} is the band gap. Values for EAs and IPs obtained in this way are also given in ESI† for comparison with IPs and EAs from calculations and electrochemical measurements. Strictly speaking this comparison is only valid at pH = PZC, but PZC is not known for a good fraction of materials considered here. However, if for a given material PZC = 10, then its band edges at PZC should according to the Nernst equation be $9 \times 0.059 = 0.53$ eV closer to the vacuum than at pH = 1. Therefore, we may consider predictions based on Mulliken electronegativities accurate if they fall by ~ 0.5 eV closer to the vacuum than the pH = 1 measured values. For the majority of the compounds considered here predicted IPs and EAs do fall by ~ 0.5 eV closer to the vacuum than the pH = 1 values from the measurements. However, in the case of InP this difference is ~ 0.8 eV and can be explained only if the PZC of InP is around pH = 14, which cannot be confirmed as the PZC value is not, to our knowledge, available in the literature.^{9,65,66} Furthermore, the difference is also very large in the case of NiO

¶ Ideally for the same surface orientation.

Table 1 Comparison of the calculated position of the valence bands of 8 materials (VBM^{theory}) and the VBM positions measured electrochemically and expressed at the pH values corresponding to the PZC for each material. Literature PZC values are also given as well as the difference $VBM^{exp.} - VBM^{theory}$. Parentheses denote ranges of values

Compound	pH _{PZC}	VBM ^{theory} [eV]	pH = pH _{PZC}	
			VBM ^{exp.} [eV]	VBM ^{exp.} - VBM ^{theory}
SnO ₂	4.3 ^{a,b} /4.19 ^c	-9.13	(-8.36, -8.00)	(0.77, 1.13)
ZnO	8.8 ^{a,b} /8.73 ^c	-7.53	(-7.31, -6.99)	(0.22, 0.54)
CdS	2 ^b /5.5 ^c	-7.15	(-6.23, -4.87)	(0.71, 2.28)
TiO ₂ ^{rut.}	5.8 ^{a,b} /5.36 ^c	-7.51	(-7.21, -6.97)	(0.30, 0.54)
TiO ₂ ^{ana.}	5.8 ^{a,b} /6.04 ^c	-7.82	(-7.21, -6.97)	(0.61, 0.85)
NiO	10.3 ^{a,b} /9.12 ^c	-4.89	(-4.78, -4.85)	(0.14, 0.20)
Cu ₂ O	8.53 ^b /5-11.5 ^c	-5.49	(-5.37, -4.99)	(0.12, 0.50)
Fe ₂ O ₃	8.6 ^{a,b} /7.61 ^{c,d}	-6.70	(-6.56, -6.50)	(0.14, 0.20)

^a Ref. 9. ^b Ref. 65. ^c Ref. 66. ^d Ref. 67.

and Cu₂O. Predicted VBM and CBM positions are closer to the vacuum than the measured ones by 1.2 and 1.8 eV, respectively, and this difference cannot be explained by their PZC values.

To estimate the magnitude of the Δ_{dipole} we compare VBM and CBM positions derived from the calculated IPs and EAs, with those measured electrochemically, but now expressed using the Nernst equation, at the pH = PZC of the corresponding material. The comparison is presented in Table 1 for the VBMs of all materials considered in this work for which the PZC values are available in the literature.^{9,65,66} Analogous results can be obtained for the CBM positions. The reality is that the reported PZC values can span a pretty large range of values, depending both on the measurement technique and the method used to grow the material.⁶⁶ For example, in the case of rutile TiO₂, it is possible to find PZC values ranging from 3.4 to about 7.0 in ref. 66, which contains a collection of measured PZC for many different materials coming from different sources. In Table 1 we use average PZC from ref. 66 and the values reported in ref. 9, 65 and 67. The last column in Table 1 lists the differences of the experimental VBM positions at pH = PZC and the VBMs derived from the calculated IPs. Relatively wide ranges of values reflect both the spread in PZC and the spread in the reported VBM positions at pH = 1.

Interestingly, all the differences are positive and average of around 0.5 eV (± 0.3 eV). Since $VBM^{exp.} - VBM^{theory}$ at pH = PZC describes the potential drop due to the dipole associated with materials interacting with H₂O molecules, this fact suggests that the band edges of materials always shift closer to the vacuum due to the presence of water, *i.e.* it requires on average ~ 0.5 eV less energy to extract an electron from the material if it is surrounded by pure water (no H⁺ and OH⁻). Given the error bars established previously, it seems that all the dependence of the interface potential drop on the actual material falls within the ± 0.3 eV range. The sign of the potential drop also implies that water conforms to the surface of a material, regardless of what material is it, in such a way that the net dipole moment always points from the surface out, in other words, more water molecules turn their oxygen side to the surface than the other way around. These findings agree very well with findings of

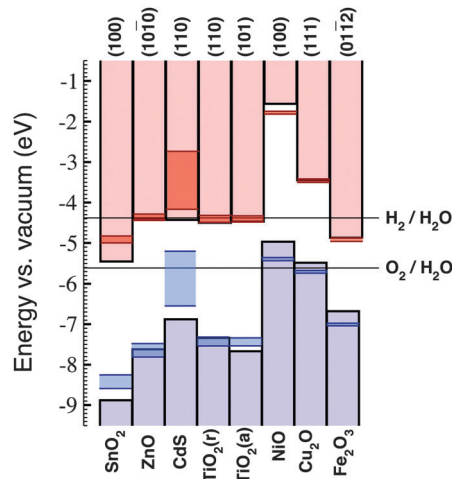


Fig. 6 Comparison of the calculated VBM and CBM positions for the compounds listed in Table 1, which are corrected for the PZC value, *i.e.* the calculated VBM and CBM are shifted 0.5 eV closer to the vacuum and then shifted back to pH = 1 using the Nernst equation and the average PZC values from Table 1. This procedure improves the quantitative agreement between the calculated VBM and CBM positions and those measured electrochemically.

Mayer *et al.*, who discovered using photomission spectroscopy a 0.6–0.7 eV decrease in the electron affinity of WSe₂, InSe and GaSe after water is adsorbed on their (0001) surface.

These findings also explain why for materials with larger PZC values band edges derived from calculated IPs and EAs compare better experimental band edges at pH = 1. Indeed, if 0.5 eV is added to the theoretical band edges and these are assumed to correspond to those in water at pH = PZC, and then using the Nernst equation transferred back to pH = 1, the addition of 0.5 eV gets completely cancelled if the value of PZC is around 10. Following this procedure improved quantitative agreement between the theoretical VBM and CBM positions and the pH = 1 measurements is achieved for all compounds from Table 1 except for Fe₂O₃, for which the prediction gets by 0.1 eV worse, but still within ~ 0.3 eV as shown in Fig. 6. In the case of CdS this procedure brings the predicted CBM at pH = 1 slightly above the water redox potential (or even ~ 0.2 eV above depending on which the PZC value is used), which corresponds better to the experimental findings that before CdS photo-corrodes evolution of H₂ gas is observed.⁶⁸ The authors of ref. 68 make the same observation for CdSe, but in the absence of the PZC value for this compound we can only say that if the PZC is around the values reported for CdS, the procedure of adding 0.5 eV to the calculated VBM and CBM and then using the Nernst equation to get from pH = PZC to pH = 1 would again result in better quantitative agreement between theory and experiment. Similarly, for GaN, GaAs, GaP and InP, better agreement between the theory and experiment would be achieved if PZC of GaN is in the range 8–10, and the PZC of GaAs, GaP and InP around 5 or below.

At the end, it is important to note that the 0.5 eV up-shift at pH = PZC brings the IPs and EAs of different materials in better quantitative agreement with the band edges measured

electrochemically and provides insight into details of the material/water interface, and that, even without this shift, the search for new water splitting materials can be guided solely using IPs and EAs.

4 Conclusions

In conclusion, we demonstrate on a set of 17 materials: (i) that direct DFT calculations of IPs and EAs of semiconductors and insulators can be corrected by the bulk GW band-edge shifts resulting in quantitative IPs and EAs, (ii) from the extensive comparison of calculated IPs and EAs with available experimental data, both from photoemission and electrochemical measurements, we show that it is possible to sort candidate water splitting materials solely from IPs and EAs, and (iii) that the effect of an aqueous environment can be approximated at $\text{pH} = \text{PZC}$ by the 0.5 eV up shift of both VBM and CBM closer to the vacuum thereby eliminating the need for explicit calculations of material/water interfaces. These results allow alignment of the semiconductor electronic bands with water reduction and oxidation potentials just on the basis of known (measured or calculated) IPs and EAs and direct assessment of the potential of semiconductors to split water.

Acknowledgements

This work was supported by the US Department of Energy, Office of Basic Energy Sciences, Energy Frontier Research Centers, under Award DE-AC36-08GO28308 to NREL. The use of high performance computing resources of NREL's Computational Science Center is gratefully acknowledged. V.S. acknowledges the administrative support of REMRSEC at Colorado School of Mines.

References

- 1 A. Fujishima and K. Honda, *Nature*, 1972, **238**, 37.
- 2 N. S. Lewis and D. G. Nocera, *Proc. Natl. Acad. Sci. U. S. A.*, 2006, **103**, 15729.
- 3 M. G. Walter, E. L. Warren, J. R. McKone, S. W. Boettcher, Q. Mi, E. A. Santori and N. S. Lewis, *Chem. Rev.*, 2012, **110**, 6446.
- 4 F. O. Osterloh and B. A. Parkinson, *MRS Bull.*, 2011, **36**, 17.
- 5 A. J. Nozik, *Annu. Rev. Phys. Chem.*, 1978, **29**, 189.
- 6 A. J. Nozik and R. Memming, *J. Phys. Chem.*, 1996, **100**, 13061.
- 7 R. J. D. Miller and R. Memming, in *Nanostructured and Photoelectrochemical Systems for Solar Photon Conversion*, ed. M. D. Archer and A. J. Nozik, Imperial College Press, London, 2008, ch. Fundamentals in photoelectrochemistry.
- 8 M. Grätzel, *Nature*, 2001, **414**, 338.
- 9 M. A. Butler and D. S. Ginley, *J. Electrochem. Soc.*, 1978, **125**, 228.
- 10 F. E. Osterloh, *Chem. Mater.*, 2008, **20**, 35.
- 11 W.-J. Yin, H. Tang, S.-H. Wei, M. M. Al-Jassim, J. Turner and Y. Yan, *Phys. Rev. B: Condens. Matter Mater. Phys.*, 2010, **82**, 045106.
- 12 W.-J. Yin, S.-H. Wei, M. M. Al-Jassim, J. Turner and Y. Yan, *Phys. Rev. B: Condens. Matter Mater. Phys.*, 2011, **83**, 155102.
- 13 I. E. Castelli, T. Olsen, S. Datta, D. D. Landis, S. Dahl, K. S. Thygesen and K. W. Jacobsen, *Energy Environ. Sci.*, 2012, **5**, 5814.
- 14 I. E. Castelli, D. D. Landis, K. S. Thygesen, S. Dahl, I. Chorkendorff, T. F. Jaramillo and K. W. Jacobsen, *Energy Environ. Sci.*, 2012, **5**, 9034.
- 15 Y. Wu, P. Lazic, G. Hautier, K. Persson and G. Ceder, *Energy Environ. Sci.*, 2013, **6**, 157.
- 16 S. Kocha, J. Turner and A. J. Nozik, *J. Electroanal. Chem.*, 1991, **367**, 27.
- 17 K. Maeda, T. Takata, M. Hara, N. Saito, Y. Inoue, H. Kobayashi and K. Domen, *J. Am. Chem. Soc.*, 2005, **127**, 8286.
- 18 K. Maeda, K. Teramura, D. Lu, T. Takata, N. Saito, Y. Inoue and K. Domen, *Nature*, 2006, **440**, 295.
- 19 C. Feng, W.-J. Yin, J. Nie, X. Zu, M. N. Huda, S.-H. Wei, M. M. Al-Jassim, J. A. Turner and Y. Yan, *Appl. Phys. Lett.*, 2012, **100**, 023901.
- 20 *Nanostructured and Photoelectrochemical Systems for Solar Photon Conversion*, ed. M. D. Archer and A. J. Nozik, Imperial College Press, London, 2008.
- 21 S. Yang, D. Prendergast and J. B. Neaton, *Nano Lett.*, 2012, **12**, 383.
- 22 S. Linic, P. Christopher and D. B. Ingram, *Nat. Mater.*, 2011, **10**, 911.
- 23 O. Khaselev and J. A. Turner, *Science*, 1998, **280**, 425.
- 24 A. Kudo, *MRS Bull.*, 2011, **36**, 32.
- 25 M. W. Kanan and D. G. Nocera, *Science*, 2008, **321**, 1072.
- 26 S. Lany, *Phys. Rev. B: Condens. Matter Mater. Phys.*, 2013, **87**, 085112.
- 27 Y. Wu, M. K. Y. Chan and G. Ceder, *Phys. Rev. B: Condens. Matter Mater. Phys.*, 2011, **83**, 235301.
- 28 M. Methfessel, D. Hennig and M. Scheffler, *Phys. Rev. B: Condens. Matter Mater. Phys.*, 1992, **46**, 4816.
- 29 H. L. Skriver and N. M. Rosengaard, *Phys. Rev. B: Condens. Matter Mater. Phys.*, 1992, **46**, 7157.
- 30 C. Sgiaravello, N. Binggeli and A. Baldereschi, *Phys. Rev. B: Condens. Matter Mater. Phys.*, 2004, **69**, 035320.
- 31 S. L. Dudarev, G. A. Botton, S. Y. Savrasov, C. J. Humphreys and A. P. Sutton, *Phys. Rev. B: Condens. Matter Mater. Phys.*, 1998, **57**, 1505.
- 32 V. Stevanović, S. Lany, X. Zhang and A. Zunger, *Phys. Rev. B: Condens. Matter Mater. Phys.*, 2012, **85**, 115104.
- 33 Springer Materials, Landolt–Börnstein Database, <http://www.springermaterials.com/docs/index.html>.
- 34 J. Paier, M. Marsman and G. Kresse, *Phys. Rev. B: Condens. Matter Mater. Phys.*, 2008, **78**, 121201(R).
- 35 G. Kresse and J. Furthmüller, *Comput. Mater. Sci.*, 1996, **6**, 15.
- 36 K. M. Tracy, W. J. Mecouch, R. F. Davis and R. J. Nemanich, *J. Appl. Phys.*, 2003, **94**, 3163.
- 37 J. Deuermeier, J. Gassmann, J. Brötz and A. Klein, *J. Appl. Phys.*, 2011, **109**, 113704.
- 38 J. Robertson and C. W. Chen, *Appl. Phys. Lett.*, 1999, **74**, 1168.
- 39 V. E. Henrich, G. Dresselhaus and H. J. Zeiger, *Phys. Rev. B: Condens. Matter Mater. Phys.*, 1978, **17**, 4908.

- 40 R. Schafrank and A. Klein, *Solid State Ionics*, 2006, **177**, 1659.
- 41 V. E. Henrich and P. A. Cox, *The Surface Science of Metal Oxide*, Cambridge University Press, Cambridge, UK, 1994.
- 42 U. Diebold, L. V. Koplitzb and O. Dulub, *Appl. Surf. Sci.*, 2004, **237**, 336.
- 43 M. Ramamoorthy, D. Vanderbilt and R. D. King-Smith, *Phys. Rev. B: Condens. Matter Mater. Phys.*, 1994, **49**, 16721.
- 44 S. Zhang, D. Tománek, S. G. Louie, M. L. Cohen and M. S. Hybertsen, *Solid State Commun.*, 1988, **66**, 585.
- 45 X. Zhu and S. G. Louie, *Phys. Rev. B: Condens. Matter Mater. Phys.*, 1991, **43**, 14142.
- 46 R. Shaltaf, G.-M. Rignanese, X. Gonze, F. Giustino and A. Pasquarello, *Phys. Rev. Lett.*, 2008, **100**, 186401.
- 47 F. Bruneval, *J. Chem. Phys.*, 2012, **136**, 194107.
- 48 R. K. Swank, *Phys. Rev.*, 1967, **153**, 844.
- 49 K. Y. Tsou and E. B. Hensley, *J. Appl. Phys.*, 1974, **45**, 47.
- 50 M. Kawasaki, K. Takahashi, T. Maeda, R. Tsuchiya, M. Shinohara, O. Ishiyama, T. Yonezawa, M. Yoshimoto and H. Koinuma, *Science*, 1994, **266**, 1540.
- 51 T. Kubo and H. Nozoye, *Surf. Sci.*, 2003, **542**, 177.
- 52 Y.-W. Chung and W. Weissbard, *Phys. Rev. B: Condens. Matter Mater. Phys.*, 1979, **20**, 3456.
- 53 B. T. Nagaraj, T. Wu, S. B. Ogale, T. Venkatesan and R. Ramesh, *J. Electroceram.*, 2002, **8**, 233.
- 54 L. F. Zagonel, M. Bäurer, A. Bailly, O. Renault, M. Hoffmann, S.-J. Shih, D. Cockayne and N. Barrett, *J. Phys.: Condens. Matter*, 2009, **21**, 314013.
- 55 A. F. Santander-Syro, O. Copie, T. Kondo, F. Fortuna, S. Pailhès, R. Weht, X. G. Qiu, F. Bertran, A. Nicolaou, A. Taleb-Ibrahimi, P. L. Fèvre, G. Herranz, M. Bibes, N. Reyren, Y. Apertet, P. Lecoeur, A. Barthélémy and M. J. Rozenberg, *Nature*, 2011, **469**, 189.
- 56 M. C. Toroker, D. K. Kanan, N. Alidoust, L. Y. Isseroff, P. Liaob and E. A. Carter, *Phys. Chem. Chem. Phys.*, 2011, **13**, 16644.
- 57 T. Bak, J. Nowotny, M. Rekas and C. C. Sorrel, *Int. J. Hydrogen Energy*, 2001, **27**, 991.
- 58 J. D. Beach, R. T. Collins and J. A. Turner, *J. Electrochem. Soc.*, 2003, **150**, A899.
- 59 Y. Matsumoto, T. Yoshikawa and E. Sato, *J. Electrochem. Soc.*, 1989, **136**, 1389.
- 60 J. He, H. Lindström, A. Hagfeldt and S.-E. Lindquist, *Sol. Energy Mater. Sol. Cells*, 2000, **62**, 265.
- 61 P. E. de Jongh, D. Vanmaekelbergh and J. J. Kelly, *J. Electrochem. Soc.*, 2000, **147**, 486.
- 62 I. Waki, D. Cohen, R. Lal, U. Mishra, S. P. DenBaars and S. Nakamura, *Appl. Phys. Lett.*, 2007, **91**, 093519.
- 63 R. Memming and G. Schwandt, *Electrochim. Acta*, 1968, **13**, 1299.
- 64 E. Aharon-Shalom and A. Heller, *J. Electrochem. Soc.*, 1982, **129**, 2865.
- 65 Y. Xu and M. A. A. Schoonen, *Am. Mineral.*, 2000, **85**, 543.
- 66 M. Kosmulski, *Surface Charging and Points of Zero Charge*, CRC Press, Boca Raton, FL, 2009.
- 67 M. Kosmulski, *J. Colloid Interface Sci.*, 2009, **337**, 439.
- 68 A. B. Ellis, S. W. Kaiser and M. S. Wrighton, *J. Am. Chem. Soc.*, 1976, **98**, 22.
- 69 A. Klein, C. Körber, A. Wachau, F. Suberlich, Y. Gassenbauer, R. Schafrank, S. Harvey and T. Mason, *Thin Solid Films*, 2009, **518**, 1197.